A Experimental setup

A.1 Training details

All models discussed in Section 5.2 were trained with 2000 iterations. If more than one learning rate was used for a certain dataset (due to problems with the convergence of individual models), all the spaces were evaluated for all learning rates, and the best result was reported for each space. For distortion, the learning rate was 0.1 for all datasets except USCA312 (Cities), where we had 0.1 and 0.01. For mAP, the learning rate 0.1 was used for all datasets except USCA312 and CSPhDs, where we had 0.01 and 0.05 for both datasets.

For the experiments in Section 5.3 , we used 5000 iterations for short embeddings and 1000 for long ones (long embeddings converged faster). Hard-negative mining was not used for DSSM training. Instead, large batches of 4096 random training examples (almost 1% of the entire dataset) were used. During the learning process, only the training queries and documents were used. For evaluation, the nearest website was searched among all the documents. The training part was 90% of the dataset, and the quality discrepancy between validation and test sets was quite small. Data samples are given in the table 11.

For the synthetic experiment in Section 5.4 , for all spaces, the learning rates 0.1, 0.05, 0.01, 0.001 were used, and the best result was selected. We had 2000 and 1000 iterations for distortion and mAP, respectively.

A.2 WLA6 dataset details

As described in the main text, this dataset is obtained by running the breadth-first search algorithm on the category graph of the English-language Wikipedia (`https://en.wikipedia.org/wiki/Special:CategoryTree`), starting from the vertex (category) "Linear algebra" and limited to the depth 6 (Wikipedia Linear Algebra 6). We provide this graph along with the texts (names) of the vertices (categories). The resulting graph is very close to being a tree, although there are some cycles. Predictably, hyperbolic space gives a significant profit for this graph, while using product spaces gives almost no additional advantage. The purpose of using this dataset is to check our conclusions on data other than those used in [9] and to evaluate overlapping spaces on a dataset where product spaces do not provide quality gains.

B Additional experimental results

B.1 Our implementation of product spaces vs original one

Table 7 compares our implementation with the results reported in [9]. It should be noted that we have significantly different algorithms with differing numbers of iterations.

The optimal values of distortion obtained with our algorithm (except for the USCA312 dataset) are comparable and usually better than those reported in [9]. On USCA312, the obtained distortion is orders of magnitude better, which can be caused by the proper choice of the learning rate (in our experiments on this dataset, this choice significantly affected the results). These results indicate that our solution is a good starting point to compare different spaces and similarities.

For mAP, we optimize the proxy-loss, in contrast to the canonical implementation, where both metrics were specified for models trained with distortion. Clearly, the results are more stable for our approach: we do not have such a large spread of values for different spaces. We noticed that directly optimizing ranking losses leads to significant improvements.

B.2 Parametrization of spherical space

In Tables 2 and 3 of the main text, we used hyperspherical parameterization of spherical subspaces in product spaces since we fixed the number of stored values for each space. Here, in Tables 8 and 9, we present the extended results, where we fix the mathematical dimension of product spaces and use $d + 1$ parameters and simple mappings from Section 3, equation (4),

Table 7: Graph reconstruction: original product spaces vs our implementation

	USCA312		CS PhDs		Power		Facebook	
	Canon.	Our	Canon.	Our	Canon.	Our	Canon.	Our
Distortion								
E_{10}	0.0735	0.0032	0.0543	0.0475	0.0917	0.0408	0.0653	0.0487
H_{10}	0.0932	0.0111	0.0502	0.0443	0.0388	0.0348	0.0596	0.0483
S_{10}	0.0598	0.0095	0.0569	0.0503	0.0500	0.0450	0.0661	0.0540
$H_5 \times H_5$	0.0756	0.0057	0.0382	0.0345	0.0365	0.0255	0.0430	0.0372
$S_5 \times S_5$	0.0593	0.0079	0.0579	0.0492	0.0471	0.0433	0.0658	0.0511
$H_5 \times S_5$	0.0622	0.0068	0.0509	0.0337	0.0323	0.0249	0.0402	0.0318
H_2^5	0.0687	0.0059	0.0357	0.0344	0.0396	0.0273	0.0525	0.0439
S_2^5	0.0638	0.0072	0.0570	0.0460	0.0483	0.0418	0.0631	0.0489
$H_2^2 \times E_2 \times S_2^2$	0.0765	0.0044	0.0391	0.0345	0.0380	0.0299	0.0474	0.0406
mAP								
E_{10}		0.9290	0.8691	0.9487	0.8860	0.9380	0.5801	0.7876
H_{10}		0.9173	0.9310	0.9399	0.8442	0.9385	0.7824	0.7997
S_{10},		0.9254	0.8329	0.9578	0.7952	0.9436	0.5562	0.7868
$H_5 \times H_5$		0.9247	0.9628	0.9481	0.8605	0.9415	0.7742	0.8084
$S_5 \times S_5$		0.9231	0.7940	0.9662	0.8059	0.9466	0.5728	0.7891
$H_5 \times S_5$		0.9316	0.9141	0.9654	0.8850	0.9467	0.7414	0.8087
H_2^5		0.9364	0.9694	0.9671	0.8739	0.9508	0.7519	0.7979
S_2^5		0.9281	0.8334	0.9714	0.8818	0.9521	0.5808	0.7915
$H_2^2 \times E_2 \times S_2^2$		0.9391	0.8672	0.9611	0.8152	0.9486	0.5951	0.7970

as done in [9]. We can see that our implementation gives results comparable to the original ones in distortion setup and significantly better for mAP, which is associated with using the proxy-loss instead of distortion.

Table 8: Graph reconstruction with distortion loss, top results are highlighted, metrics only

Signature	**USCA312**	**CS PhDs**	**Power**	**Facebook**	**WLA6**
E_{10}	**0.00318**	0.0475	0.0408	0.0487	0.0530
H_{10}	0.01114	0.0443	0.0348	0.0483	**0.0279**
S_{10}	0.00951	0.0503	0.0450	0.0540	0.0589
$H_5^2 \equiv H_5 \times H_5$	0.00573	0.0345	0.0255	0.0372	**0.0279**
$S_5 \times S_5 \equiv S_5^2$	0.00792	0.0492	0.0433	0.0511	0.0585
$H_5 \times S_5$	0.00681	**0.0337**	**0.0249**	**0.0318**	0.0296
H_2^5	0.00592	0.0344	0.0273	0.0439	0.0356
S_2^5	0.00720	0.0460	0.0418	0.0489	0.0549
$H_2^2 \times E_2 \times S_2^2$	0.00436	0.0345	0.0299	0.0406	0.0405
$O_{l1}, t = 0$	**0.00356**	0.0368	0.0281	0.0458	0.0286
$O_{l1}, t = 1$	**0.00330**	**0.0300**	**0.0231**	**0.0371**	**0.0272**
$O_{l2}, t = 1$	0.00530	**0.0328**	**0.0246**	**0.0324**	**0.0278**

Table 10: Comparison of proxy-losses, mAP

	USCA312			**CS PhD**		
$P \sim$	e^{-d}	$e^{1/d}$	$1/d$	e^{-d}	$e^{1/d}$	$1/d$
E_{10}	0.929	0.911	0.899	0.949	0.956	0.831
H_{10}	0.917	0.807	0.885	0.940	0.749	0.764
S_{10}	0.925	0.797	0.838	0.958	0.572	0.689
H_5^2	0.925	0.890	0.883	0.948	0.976	0.723
S_5^2	0.923	0.802	0.858	0.966	0.748	0.775
$H_5 \times S_5$	0.932	0.838	0.865	0.965	0.804	0.721
H_2^5	0.936	0.896	0.903	0.967	0.998	0.823
S_2^5	0.928	0.856	0.871	0.971	0.876	0.881
$H_2^2 \times E_2 \times S_2^2$	0.939	0.872	0.865	0.961	0.884	0.689
$O_{l1}, t = 0$	0.952	0.933	0.872	0.988	0.961	0.762
$O_{l1}, t = 1$	0.952	0.947	0.877	0.990	0.963	0.815
$O_{l2}, t = 1$	0.952	0.939	0.880	0.994	0.979	0.810
$c-$ dot	1	1	0.777	1	0.999	0.917

Table 9: Graph reconstruction with mAP ranking loss, top results are highlighted, metrics only

Signature	**USCA312**	**CS PhDs**	**Power**	**Facebook**	**WLA6**
E_{10}	0.9290	0.9487	0.9380	0.7876	0.7199
H_{10}	0.9173	0.9399	0.9385	0.7997	0.9617
S_{10}	0.9254	0.9578	0.9436	0.7868	0.7287
H_5^2	0.9247	0.9481	0.9415	0.8084	**0.9682**
S_5^2	0.9231	0.9662	0.9466	0.7891	0.7353
$H_5 \times S_5$	0.9316	0.9654	0.9467	0.8087	**0.9779**
H_2^5	0.9364	0.9671	0.9508	0.7979	0.8597
S_2^5	0.9281	0.9714	0.9521	0.7915	0.7346
$H_2^2 \times E_2 \times S_2^2$	0.9391	0.9611	0.9486	0.7970	0.6796
$O_{l1}, t = 0$	**0.9522**	**0.9879**	**0.9728**	**0.8093**	0.6759
$O_{l1}, t = 1$	**0.9522**	**0.9904**	**0.9762**	**0.8185**	0.9598
$O_{l2}, t = 1$	**0.9522**	**0.9938**	**0.9907**	**0.8326**	**0.9694**

B.3 Other ways of converting distances to probabilities

For the proxy-loss, we additionally experimented with other ways of converting distances to probabilities. Let us write L_{proxy} in the general form:

$$L_{proxy} = -\sum_{(v,u)\in E} \log \mathrm{P}((v,u)\in E) = -\sum_{(v,u)\in E} \log \frac{t\big(d_U(f(v), f(u))\big)}{\sum\limits_{w\in V} t\big(d_U(f(v), f(w))\big)}, \tag{7}$$

where $t(d)$ is a function that decreases with distance d. We compare the following alternatives for $t(d)$:

$$t_1(d) = \exp(-d), t_2(d) = \exp\left(\frac{1}{\min(d, d_0)}\right), t_3(d) = \frac{1}{\min(d, d_0)},$$

where d_0 is a small constant.

Recall that t_1 was used in the main text and it seems to be the most natural choice.[10] Table 10 compares the options and shows that the best results are indeed achieved with t_1.

[10]Note that this is the softmax over the inverted distances.

Table 11: Search query examples

Query	Web site
Kris Wallace	en.wikipedia.org/wiki/Chris_Wallace
1980: Mitsubishi produces one million cars...//	en.wikipedia.org/wiki/Mitsubishi_Motors
code napoleon	en.wikipedia.org/wiki/Napoleonic_Code

Table 12: Distortion graph reconstruction for different overlapping spaces

Signature	USCA312	CS PhDs	Power	Facebook	WLA6	EuCore
$O_{l1}, t = 0$	0.00324	0.0368	0.0281	0.0458	0.0286	0.1141
$O_{l1}, t = 1$	0.00325	0.0300	0.0231	0.0371	0.0272	0.1117
$O_{l1}, t = 2$	0.00296	0.0335	0.0262	0.0309	0.0273	0.1114
$O_{l1}, t = 3$	0.00257	0.0273	0.0209	0.0313	0.0246	0.1098
$O_{l2}, t = 1$	0.00530	0.0328	0.0246	0.0324	0.0278	0.1127
$O_{l2}, t = 2$	0.00596	0.0303	0.0256	0.0312	0.0278	0.1117
$O_{l2}, t = 3$	0.00303	0.0343	0.0240	0.0302	0.0279	0.1119

B.4 Analysis of depth in overlapping spaces

Distortion graph reconstruction results for all possible $t \leq \log_2(d) = \log_2(10) \sim 3.3$ are provided in Table 12 for completeness. The results below confirm our hypothesis that the reconstruction distortion improves with increasing t.

B.5 Analysis of learned weights

While analyzing the trained weights we have made several observations:

1. We see that OS does not learn a pure product space. In particular, on the CS PhDs dataset we get
$$d_{O_{l=1},t=0} \propto 0.37 d_H + 0.63 d_S,$$
which is significantly better than both d_S and d_H separately.
2. If for $t = 0$ there is a space with a noticeably larger weight compared to the other ones, then the space of same type often makes the largest contribution for $t = 1$ too. For example, in USCA312,
$$d_{O_{l1},t=0} \propto \mathbf{0.90} d_E + 0.05 d_H + 0.05 d_S,$$
and the weights of the Euclidean subdistances for $d_{O_{l1},t=1}$ (normalized, $\sum w_i = 1$) are 0.6, 0.15, 0.1.
3. However, a space that is absent for $t = 0$ can appear for $t = 1$. For example, in the Power dataset,
$$d_{O_{l1},t=0} \propto 0.37 d_H + 0.63 d_S,$$
$$d_{O_{l1},t=1} \propto \mathbf{0.1} d_E(l_1^0, r_1^0) + 0.5 d_R(l_1^0, r_1^0) + 0.4 d_H(l_1^1, r_1^1),$$
where $l_1^0 = l[0..5], l_1^1 = l[6..10]$.
4. Finally, we noticed that almost always, more than half of the weights are near-zero, which allows one to remove unnecessary distances and improve efficiency.

C Proof of Statement 1

To prove that $d(x, y)$ is a metric distance, we need to show that it is symmetric, nonnegative, equals zero only when $x = y$, and satisfies the triangle inequality.

Consider an overlapping space:

$$d_O(l, r) = \mathrm{Agg}(d_{D_1}(\cdot, \cdot), \ldots, d_{D_k}(\cdot, \cdot)),$$

where Agg is $l1$ or $l2$ aggregation and d_{D_i} are base distances applied to subsets of coordinates.

Symmetry of d_O follows from symmetry of base distances d_{D_i}. Obviously, we have $d_O(x,y) \geq 0$ and $d_O(x,x) = 0$. The inequality $d_O(x,y) > 0$ for $x \neq y$ follows from the fact hat we use specific non-trival mappings M_{D_i} and assume that together subsets of coordinates p_i cover all coordinates (i.e., $\cup_{i=1}^k p_i = \{1, \ldots, d\}$).

Obviously, $l1$ aggregation (sum) preserves the triangle inequality. So, it remains to show this for $l2$. Assume that d_1 and d_2 satisfy the triangle inequality, nonnegative and let $d_{l2} = \sqrt{d_1^2 + d_2^2}$.

Let $c_1 := d_1(x,y)$, $c_2 := d_2(x,y)$, $a_1 = d_1(x,z)$, $a_2 = d_2(x,z)$, $b_1 = d_1(z,y)$, $b_2 = d_2(z,y)$.

We know that $c_1 \leq a_1 + b_1$ and $c_2 \leq a_2 + b_2$. Therefore,

$$c_1^2 + c_2^2 \leq a_1^2 + a_2^2 + b_1^2 + b_2^2 + 2a_1b_1 + 2a_2b_2 \,. \tag{8}$$

We need to show

$$\sqrt{c_1^2 + c_2^2} \leq \sqrt{a_1^2 + a_2^2} + \sqrt{b_1^2 + b_2^2}\,,$$

$$c_1^2 + c_2^2 \leq a_1^2 + a_2^2 + b_1^2 + b_2^2 + 2\sqrt{a_1^2 + a_2^2}\sqrt{b_1^2 + b_2^2}\,.$$

Taking into account Equation 8, it is sufficient to show

$$2a_1b_1 + 2a_2b_2 \leq 2\sqrt{a_1^2 + a_2^2}\sqrt{b_1^2 + b_2^2}\,,$$

$$a_1^2b_1^2 + a_2^2b_2^2 + 2a_1b_1a_2b_2 \leq (a_1^2 + a_2^2)(b_1^2 + b_2^2)\,,$$

$$2a_1b_1a_2b_2 \leq a_1^2b_2^2 + a_2^2b_1^2\,,$$

which is true.

Finally, note that that for three base distances we have $d_{l2} = \sqrt{(\sqrt{d_1^2 + d_2^2})^2 + d_3^2} = \sqrt{d_1^2 + d_2^2 + d_3^2}$ and so we have proved the statement for an arbitrary number of terms.

D Additional illustrations for overlapping spaces

Figure 3 additionally illustrates the idea behind overlapping spaces. Namely, Figure 3(a) shows standard Euclidean distance evaluation between two vectors l and r. As shown in Figure 3(b), we add a differentiable mapping $M_H : \mathbb{R}^{10} \to H_{10}$ to calculate the distance in the hyperbolic space (we may do the same for the spherical space). Applying several mappings to different parts of l and r, we may get any product space as shown in Figure 3(c). The last step is to allow the subsets of coordinates to *overlap*, as shown in Figure 3(d), where the fifth coordinate is used simultaneously in two mappings. All such spaces with all possible intersections and base distances are called overlapping spaces.

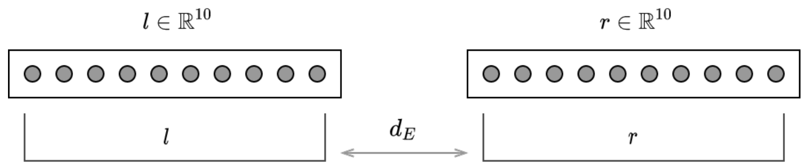

$$d_E^2(l,r) = \sum_{i=1}^{10}(l_i - r_i)^2$$

(a) Computing Euclidean distance

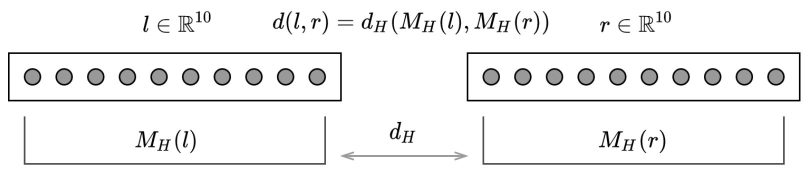

(b) Computing hyperbolic distance

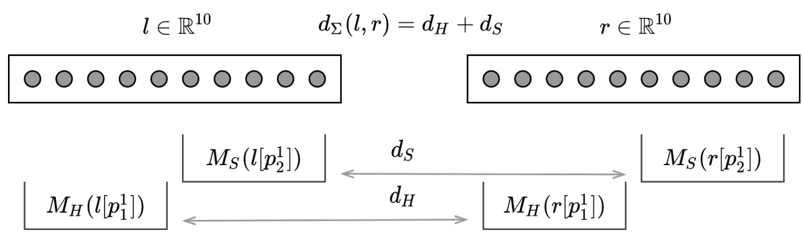

(c) Computing product space distance

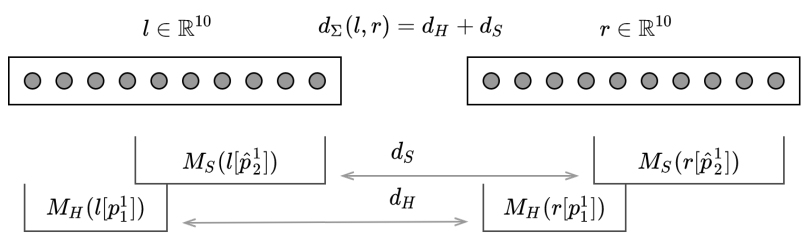

(d) Example of overlapping space distance

Figure 3: Illustrating overlapping space with $d = 10$ and $l1$ (sum) aggregation

References

[1] Phillip Bonacich. 2008. Book Review: W. de Nooy, A. Mrvar, and V. Batagelj Exploratory Social Network Analysis With Pajek. (2004). *Sociological Methods & Research - SOCIOL METHOD RES* 36 (05 2008), 563–564. https://doi.org/10.1177/0049124107306674

[2] Silvere Bonnabel. 2013. Stochastic Gradient Descent on Riemannian Manifolds. *IEEE Trans. Automat. Control* 58 (2013), 2217–2229.

[3] Jane Bromley, Isabelle Guyon, Yann LeCun, Eduard Säckinger, and Roopak Shah. 1994. Signature verification using a" siamese" time delay neural network. In *Advances in neural information processing systems*. 737–744.

[4] John Burkardt. 2011. Cities – City Distance Datasets. https://people.sc.fsu.edu/~jburkardt/datasets/cities/cities.html

[5] Frederick Arthur Ficken. 1939. The Riemannian and affine differential geometry of product-spaces. (1939), 892–913.

[6] Palash Goyal and Emilio Ferrara. 2018. Graph embedding techniques, applications, and performance: A survey. *Knowledge-Based Systems* 151 (2018), 78–94. https://doi.org/10.1016/j.knosys.2018.03.022

[7] Mihajlo Grbovic, Vladan Radosavljevic, Nemanja Djuric, Narayan Bhamidipati, Jaikit Savla, Varun Bhagwan, and Doug Sharp. 2015. E-commerce in your inbox: Product recommendations at scale. In *Proceedings of the 21th ACM SIGKDD international conference on knowledge discovery and data mining*. 1809–1818.

[8] Aditya Grover and Jure Leskovec. 2016. node2vec: Scalable Feature Learning for Networks. *CoRR* abs/1607.00653 (2016). arXiv:1607.00653 http://arxiv.org/abs/1607.00653

[9] Albert Gu, Frederic Sala, Beliz Gunel, and Christopher Ré. 2019. Learning mixed-curvature representations in product spaces. *International Conference on Learning Representations (ICLR)* (2019).

[10] Yifan Hu, Yehuda Koren, and Chris Volinsky. 2008. Collaborative Filtering for Implicit Feedback Datasets. In *IEEE International Conference on Data Mining (ICDM 2008)*. 263–272. http://yifanhu.net/PUB/cf.pdf

[11] Po-Sen Huang, Xiaodong He, Jianfeng Gao, Li Deng, Alex Acero, and Larry Heck. 2013. Learning Deep Structured Semantic Models for Web Search using Clickthrough Data. ACM International Conference on Information and Knowledge Management (CIKM).

[12] Valentin Khrulkov, Leyla Mirvakhabova, Evgeniya Ustinova, Ivan Oseledets, and Victor Lempitsky. 2020. Hyperbolic image embeddings. In *Proceedings of the IEEE/CVF Conference on Computer Vision and Pattern Recognition*. 6418–6428.

[13] Geewook Kim, Akifumi Okuno, Kazuki Fukui, and Hidetoshi Shimodaira. 2019. Representation learning with weighted inner product for universal approximation of general similarities. *arXiv preprint arXiv:1902.10409* (2019).

[14] Diederik Kingma and Jimmy Ba. 2014. Adam: A Method for Stochastic Optimization. *International Conference on Learning Representations* (12 2014).

[15] Marc Teva Law, Renjie Liao, Jake Snell, and Richard S. Zemel. 2019. Lorentzian Distance Learning for Hyperbolic Representations. In *ICML*.

[16] Jure Leskovec, Jon Kleinberg, and Christos Faloutsos. 2007. Graph evolution: Densification and shrinking diameters. *ACM transactions on Knowledge Discovery from Data (TKDD)* 1, 1 (2007), 2–es.

[17] Jure Leskovec and Julian J. Mcauley. 2012. Learning to Discover Social Circles in Ego Networks. In *Advances in Neural Information Processing Systems 25*, F. Pereira, C. J. C. Burges, L. Bottou, and K. Q. Weinberger (Eds.). Curran Associates, Inc., 539–547. http://papers.nips.cc/paper/4532-learning-to-discover-social-circles-in-ego-networks.pdf

[18] Weiyang Liu, Yandong Wen, Zhiding Yu, Ming Li, Bhiksha Raj, and Le Song. 2017. Sphereface: Deep hypersphere embedding for face recognition. In *Proceedings of the IEEE conference on computer vision and pattern recognition*. 212–220.

[19] Tomas Mikolov, Kai Chen, Greg Corrado, and Jeffrey Dean. 2013. Efficient Estimation of Word Representations in Vector Space. *CoRR* abs/1301.3781 (2013). http://dblp.uni-trier.de/db/journals/corr/corr1301.html#abs-1301-3781

[20] Maximillian Nickel and Douwe Kiela. 2017. Poincaré embeddings for learning hierarchical representations. In *Advances in neural information processing systems*. 6338–6347. http://papers.nips.cc/paper/7213-poincare-embeddings-for-learning-hierarchical-representations.pdf

[21] Maximillian Nickel and Douwe Kiela. 2018. Learning Continuous Hierarchies in the Lorentz Model of Hyperbolic Geometry. In *International Conference on Machine Learning*. 3776–3785. https://arxiv.org/abs/1806.03417

[22] Jeffrey Pennington, Richard Socher, and Christopher D. Manning. 2014. GloVe: Global Vectors for Word Representation. In *Empirical Methods in Natural Language Processing (EMNLP)*. 1532–1543. http://www.aclweb.org/anthology/D14-1162

[23] Bryan Perozzi, Rami Al-Rfou, and Steven Skiena. 2014. DeepWalk: Online Learning of Social Representations. *CoRR* abs/1403.6652 (2014). arXiv:1403.6652 http://arxiv.org/abs/1403.6652

[24] Gang Qian, Shamik Sural, Yuelong Gu, and Sakti Pramanik. 2004. Similarity between Euclidean and Cosine Angle Distance for Nearest Neighbor Queries. In *Proceedings of the 2004 ACM Symposium on Applied Computing (SAC '04)*. Association for Computing Machinery, New York, NY, USA, 1232–1237. https://doi.org/10.1145/967900.968151

[25] Frederic Sala, Chris De Sa, Albert Gu, and Christopher Re. 2018. Representation Tradeoffs for Hyperbolic Embeddings. In *International Conference on Machine Learning*. 4457–4466.

[26] Alexandru Tifrea, Gary Bécigneul, and Octavian-Eugen Ganea. 2018. Poincar\'e GloVe: Hyperbolic Word Embeddings. *arXiv preprint arXiv:1810.06546* (2018).

[27] Pavan K Turaga and Anuj Srivastava. 2016. *Riemannian Computing in Computer Vision.* Springer.

[28] Steven H Watts, Duncan J./Strogatz. 1998. *Collective Dynamics of Small- World Networks. Nature*. 393:440 – 442. https://doi.org/10.1007/978-3-658-21742-6_130

[29] Benjamin Wilson and Matthias Leimeister. 2018. Gradient descent in hyperbolic space. *arXiv preprint arXiv:1805.08207* (2018).

[30] Richard C Wilson, Edwin R Hancock, Elżbieta Pekalska, and Robert PW Duin. 2014. Spherical and hyperbolic embeddings of data. *IEEE transactions on pattern analysis and machine intelligence* 36, 11 (2014), 2255–2269.